Time Domain Simulation and Characterisation of TEM Horns Using Normalised Impulse Response

Bart Scheers, Marc Acheroy and André Vander Vorst

Abstract

A common way of describing antennas in the time domain is by means of their impulse response. When the time domain antenna equations are expressed in terms of the normalised impulse response (normalised IR), they become very simple to use, because all frequency dependent antenna characteristics are included in the normalised IR. This paper describes a method for measuring the normalised IR experimentally, using a vector network analyser. The normalised IRs of different air and dielectric-filled TEM horn antennas are compared and discussed. The normalised IR is found to be a powerful tool for simulating antenna behaviour directly in the time domain. Thanks to the introduction of the virtual source, (i.e. an apparent point in the antenna from which the radiated field degrades by a factor 1/r), the time domain antenna equations can also be used near the TEM horns, although still in the far field of the antenna. Some examples of time domain simulations and system modelling using the normalised IR are presented. In each example, the simulations are compared with measured data.

1. INTRODUCTION

In an effort to increase the directivity or the antenna gain for a broadband and non-dispersive antenna, many researchers have considered a TEM horn. A travelling wave TEM horn consists of a pair of triangular conductors forming a V structure, capable of radiating and receiving a fast transient pulse [1]. It is assumed that the TEM horn guides essentially the TEM mode within the frequency range of interest by maintaining a constant characteristic impedance and that, by neglecting the edge diffraction effect, a linearly polarised spherical wave is radiated.

The conventional design of the TEM horn is based on the infinitely long biconical antenna [2][3]. Many variants are possible, e.g. resistive loading of the antenna [4], tapering the antenna plates, gradually changing the separation angle between the antenna plates [5], placing a dielectric lens at the aperture [6], and filling the whole antenna with a dielectric [7]. The question is how to compare performances of these different variants of TEM horns.

When using TEM horn antennas, classical antenna parameters such as gain, radiation pattern, and phase centre, have less meaning [8]. All these parameters are frequency dependent, hence they have to be expressed over the whole frequency band of interest. As time domain antennas have intrinsically a large bandwidth, describing the antenna performances with the frequency dependent parameters is complicated. On the other hand, other antenna parameters become more important for time domain antennas, such as ringing in the antenna, antenna bandwidth, and the capability of radiating a clean pulse. These are all important parameters for applications in the field of ultra-wideband radar systems, where the performance often depends on the quality of the raw data prior to processing. Furthermore, there is a need for describing the antenna performances in a compact way, which can be used for modelling, or for comparing performances of different time domain antennas.

A common way of describing systems in the time domain is by means of an impulse response (IR), which is the equivalent of the transfer function in the frequency domain. The IR completely describes the linear time-invariant system.

2. TIME DOMAIN ANTENNA EQUATIONS

In this section, the antenna equations are first expressed in terms of conventional IR and later (Section 2.C) in terms of normalised IR. To simplify the expressions, we only consider antenna performance on boresight for dominant linear polarisation of the E-field. The extension to the more general case is possible however, without too much effort. Further we consider the input and output impedance of the equipment used, matched to 50 Ω (denoted Z_c). We define V_s as the voltage generated by the source in a 50 Ω load and V_{rec} as the voltage measured by an oscilloscope with a 50 Ω input impedance.

A. Transmitting antenna

First consider the case of the transmitting antenna, near the coordinate origin $\vec{r} = \vec{0}$. As input we consider a voltage V_s applied at the input reference plane (Fig. 1).

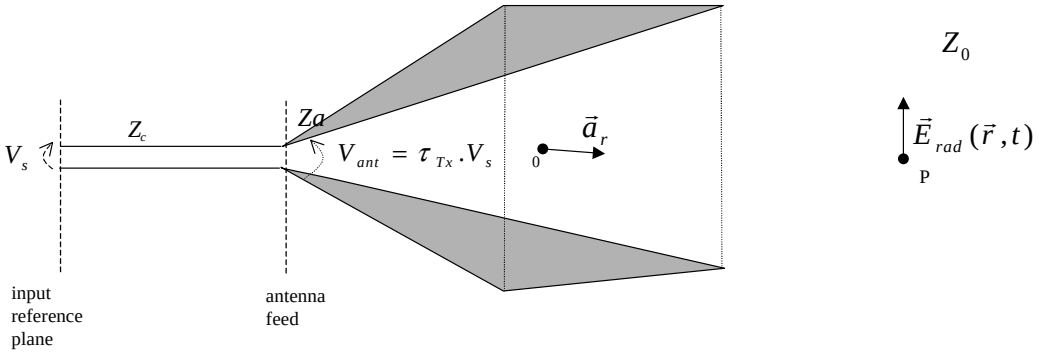

Figure 1: Transmitting antenna configuration

The radiated field $\vec{E}_{rad}(\vec{r},t)$ in a point P in the far field, for $\vec{r} \to \infty$, can be described as [9][10]:

$$\vec{E}_{rad}(\vec{r},t) = \frac{1}{2\pi r c f_g} \frac{d\vec{h}_{Tx}(\vec{a}_r,t)}{dt} \otimes V_{ant}(t) \otimes \delta(t - t_{d,TX}) \qquad \textbf{(2. 1)}$$

with $V_{ant} = \tau_{Tx} V_s$, $\tau_{Tx} = \frac{2Z_a}{Z_c + Z_a}$, $f_g = \frac{Z_a}{Z_0}$

where r is defined to be $r = |\vec{r}|$, $\vec{a}_r = \frac{\vec{r}}{|\vec{r}|}$, V_{ant} is the excitation voltage at the antenna feed, τ_{Tx} the voltage transmission coefficient from the feed cable to the antenna, Z_a the antenna input impedance, assumed to be a real constant, and $Z_0 = 120\pi$. The convolution with the dirac-function $\delta(t - t_{d,TX})$ in (2.1) introduces a total delay $t_{d,TX}$, which corresponds to the propagation time between the input of the antenna system where V_s is applied (input reference plane) and the observation point P where $\vec{E}_{rad}(\vec{r},t)$ is evaluated.

For uniformity reasons, we use $\vec{h}_{Tx}$ as kernel for the convolution in (2.1) and derive the input signal V_s. Taking into account the simplification of working only on boresight for dominant linear polarisation of the E-field, (2.1) can than be rewritten as:

$$E_{rad}(r,t) = \frac{\tau_{Tx}}{2\pi r c f_g} h_{Tx}(t) \otimes \frac{dVs(t)}{dt} \otimes \delta(t - t_{d,TX}) \qquad \textbf{(2. 2)}$$

As discussed in [10], for finite $r = |\vec{r}|$, one should limit the highest frequency for such result to be valid. Recognising these limitations, we introduce another problem. Due to the finite but non-zero dimension of the antenna, the location of the coordinate system origin $\vec{r} = \vec{0}$ becomes ambiguous. To solve this, let us define an apparent point in the antenna from which the radiated field $E_{rad}(r,t)$ degrades with a factor 1/r (free space loss) in the far field. We call this point the "virtual source" of the antenna. It can be considered as the origin of the radiated impulse TEM wave. Assuming that the position of the virtual source is frequency independent over the frequency band of interest (this has been verified experimentally for a dielectric filled TEM horn), it can easily be located. The virtual source will in general be located between the antenna feed and the aperture. When defining the origin of the coordinate system $\vec{r} = \vec{0}$ in this point, equation (2.2) is valid for finite $r = |\vec{r}|$.

A disadvantage of using expression (2.2) is that Z_a is a function of frequency, so τ_{Rx} and f_g are not constant. It will be shown that this difficulty can be eliminated by introducing a normalised IR.

B. Receiving antenna

Consider now the case of the receiving antenna, with a uniform plane-wave incident E-field $\vec{E}_{inc}(\vec{r},t)$, evaluated in the virtual source point of the receiving antenna (Fig. 2).

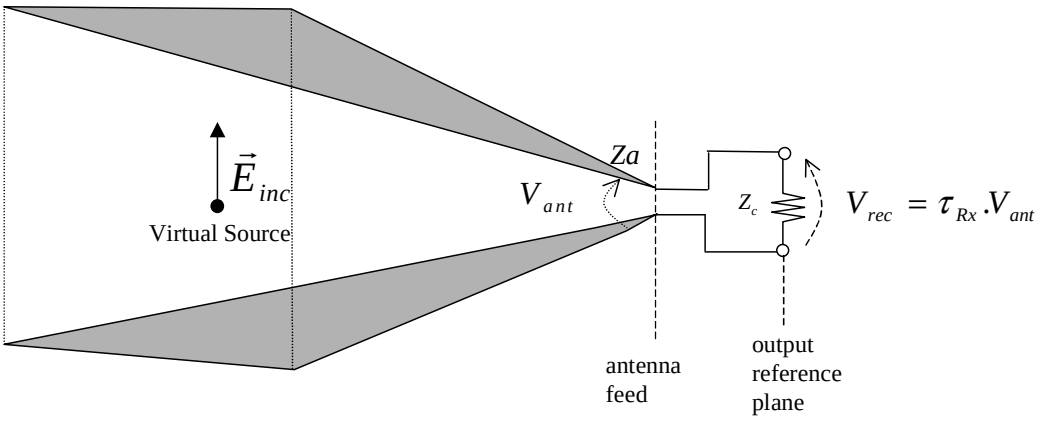

Figure 2: Receiving antenna configuration

Considering the direction of incidence to be at boresight for dominant polarisation, the output voltage $V_{rec}(t)$ measured by an oscilloscope in the output reference plane is related to the incident field by [9][10]:

$$V_{rec}(t) = \tau_{Rx}\, h_{Rx}(t) \otimes E_{inc}(t) \otimes \delta(t - t_{d,RX}) \qquad \textbf{(2. 3)}$$

$$\text{with} \quad \tau_{Rx} = \frac{2Z_c}{Z_c + Z_a}$$

where h_{Rx} is the impulse response of the receiving antenna at boresight incidence for dominant polarisation, and $t_{d,RX}$ represents the total propagation time between the virtual source point of the receiving antenna and the output reference plane where $V_{rec}(t)$ is measured.

Note that according to the Rayleigh-Carson reciprocity theorem, the ratio of the transmit frequency response function of an antenna to the receive frequency response function of the same antenna, is proportional to frequency [1]. So the IR of the transmitting antenna has to be proportional to the time derivative of the IR of the receiving antenna. This can be seen by comparing expression (2.1) and (2.3). Expressions (2.2) and (2.3) are defined such that, if the transmitting and receiving antennas are the same, $h_{Rx} = h_{Tx}$.

C. Normalisation of the IR

The disadvantage of using expressions (2.2) and (2.3) is that in reality Z_a is a function of frequency, so that τ_{Rx} and f_g are not a constant. It would be logical and easier to integrate this frequency dependent term Z_a in the IR, which is in any event unique for each antenna. This can be done by normalising expressions (2.2) and (2.3), as proposed in [9]. When normalising, in the antenna equations, the voltages and electric fields to the local characteristic impedance, the normalised IRs $h_{N,Tx}$ and $h_{N,Rx}$ can be defined as:

$$h_{N,Tx} = \sqrt{\frac{Z_c}{Z_a}} \frac{\tau_{Tx}}{\sqrt{f_g}} h_{Tx} \quad \text{and} \quad h_{N,Rx} = \sqrt{\frac{Z_a}{Z_c}} \frac{\tau_{Rx}}{\sqrt{f_g}} h_{Rx} \qquad \textbf{(2.4)}$$

Expressions (2.2) and (2.3) can be rewritten as:

$$\boxed{\frac{E_{rad}(r,t)}{\sqrt{Z_0}} = \frac{1}{2\pi r c} \; h_{N,Tx}(t) \otimes \frac{1}{\sqrt{Z_c}} \frac{dVs(t)}{dt} \otimes \delta(t - t_{d,TX})} \qquad \textbf{(2. 5)}$$

$$\boxed{\frac{V_{rec}(t)}{\sqrt{Z_c}} = h_{N,Rx}(t) \otimes \frac{E_{inc}(t)}{\sqrt{Z_0}} \otimes \delta(t - t_{d,RX})} \qquad \textbf{(2. 6)}$$

If the transmitting and receiving antenna are the same, than $h_{N,Rx} = h_{N,Tx}$. Combining expressions (2.5) and (2.6), the received voltage, measured with a 50 ohm oscilloscope at the receiving antenna, can be related to the input voltage by:

$$\boxed{V_{rec}(t) = \frac{1}{2\pi R c} h_{N,Tx}(t) \otimes h_{N,Rx}(t) \otimes \frac{dVs(t)}{dt} \otimes \delta(t - t_{d,TX} - t_{d,RX})} \qquad \textbf{(2. 7)}$$

where R is defined as the distance between the two virtual points of the antennas at boresight, and $t_{d,TX} + t_{d,RX}$ represents the total delay in the combined system. This delay is of importance for the measurement of the normalised impulse response.

Expressions (2.5), (2.6) and (2.7) are extremely simple. They can be used without any assumption about the frequency dependent antenna impedance. Knowing the normalised IR of the antennas, one can calculate, as a function of the input signal, the exact radiated E-field at any point P in the far field on boresight of the transmitting antenna. One can also calculate the received voltage for an incoming E-field.

3. MEASUREMENT OF THE NORMALISED IR

Before measuring the normalised IR of an antenna, we first have to locate the virtual source of the antenna. This can be done experimentally by using two identical antennas on boresight. The virtual source can be seen as the origin of the radiated impulse, from which the 1/R free space loss is initiated. Let d be the distance between the two antenna apertures, which is easy to measure. For different values of d, the measured voltage V_{rec} degrades with 1/R in the far field.

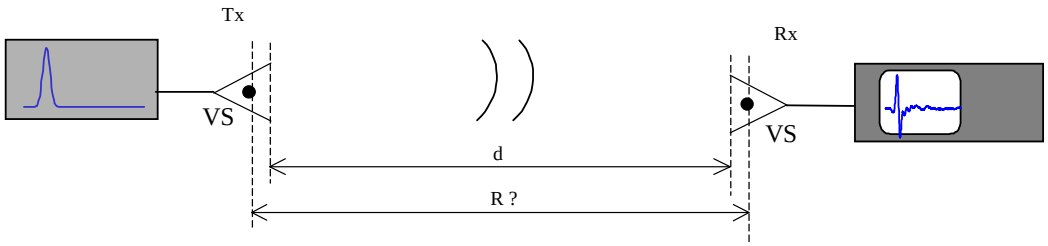

Figure 3: Set-up for locating the virtual source (VS) of an antenna

In Figure 4 we present d versus the inverse peak-to-peak value of the received voltage V_{rec}. The zero of the line fitted through these points in the least-squares sense gives the difference between R and d. In this example (R - d) is 8 cm, so the virtual source is located at 4 cm from the antenna aperture towards the antenna feed. The knowledge of the exact location of the virtual source is important when

(2.5), (2.6) or (2.7) are used near the antennas (but still in the far field) or for exact measurement of the normalised IR of an antenna.

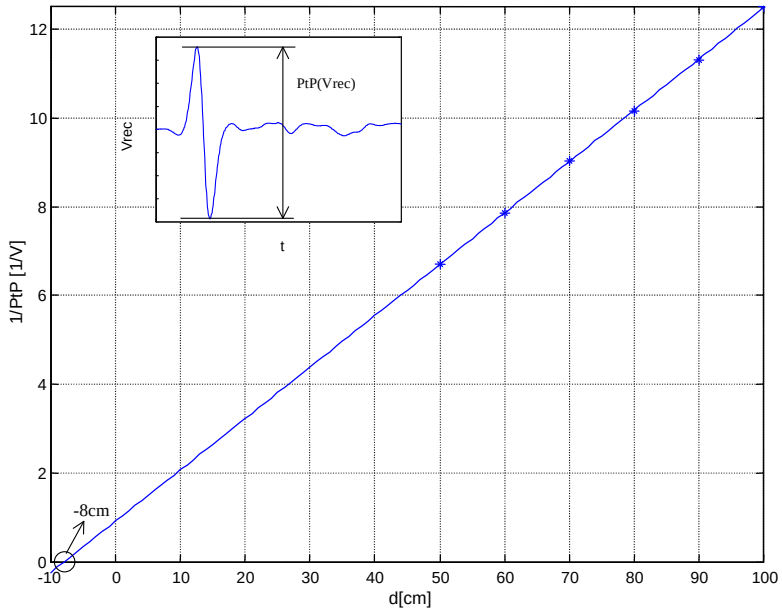

Figure 4: d versus the inverse point to point value of the received voltage V_{rec}

Now $h_{N,Tx}$ and $h_{N,Rx}$ can be measured, by using two identical antennas and a vector network analyser (VNA). Converting (2.7) into the frequency domain, the normalised transfer function of the antennas is expressed as:

$$H_N(\omega) = \sqrt{\frac{2\pi R c V_{rec}(\omega)}{j\omega V_s(\omega)}} e^{j\omega(t_{d,TX}+t_{d,RX})} \qquad \textbf{(3.1)}$$

Considering the two antennas on boresight in the far field, with a distance R between the two virtual sources, as a two-port, one can measure the S12 parameter with a VNA over the frequency band of interest, covering at least the whole frequency range of the antenna.

The quantity $t_{d,TX} + t_{d,RX}$, total delay between the reference planes of port 1 and port 2, can be replaced by $\frac{R'}{c}$, where R' is the distance between the two reference planes of the VNA and c the speed of light.

Expression (3.1) can then be written as:

$$H_N(\omega) = \sqrt{\frac{2\pi R c}{j\omega} S_{12}(\omega) e^{j\omega R'/c}} \qquad \textbf{(3.2)}$$

In expression (3.2) the square root is taken from a complex number. To do so, one first has to unwrap the phase, otherwise the result is non-physical. The unwrapping is far more easy by taking into account the term $e^{j\omega R'/c}$, hence its importance.

Once the frequency vector $H_N(\omega)$ is found, $h_N(t)$ can be extracted by a frequency-time transformation [11]. The desired time resolution of the IR is obtained by zeropadding the frequency vector.

4. RESULTS ON TEM HORNS

The normalised IR describes the antenna performances in a very compact way. In this section the performances on boresight of four different TEM horns are compared. Table 4.1 summarises the physical characteristics of the tested antennas. (L is the length of the antenna plates and A_{ap} the area of the antenna aperture).

	L (cm)	A_{ap} (cm²)	Filling
Antenna 1	10	10*4	air
Antenna 2	10	10*4	dielectric
Antenna 3	12	12*6	dielectric
Antenna 4	12	12*6	dielectric

Table 4.1: The physical characteristics of the tested antennas

Antenna 1 is a conventional air-filled TEM horn. Antennas 2, 3 and 4 are filled with a dielectric to increase their electrical size. The dielectric is characterised by a real relative dielectric constant of $\varepsilon_r \approx 3$ and a loss tangent of 0.0084 at 1 GHz. Antenna 4 is the same as antenna 3 but an absorber is placed at the outside end of the antenna plates to reduce the current at the end of the antenna plates.

For each antenna, S12 was measured between 40 MHz and 20 GHz, with a frequency step of 40 MHz, by placing two identical antennas on boresight. The normalised IRs of the antennas are shown in Figure 5. Note that the dimensions of $h_N(t)$ are given in m/ns, which corresponds with the dimensions needed in (2.5) and (2.6).

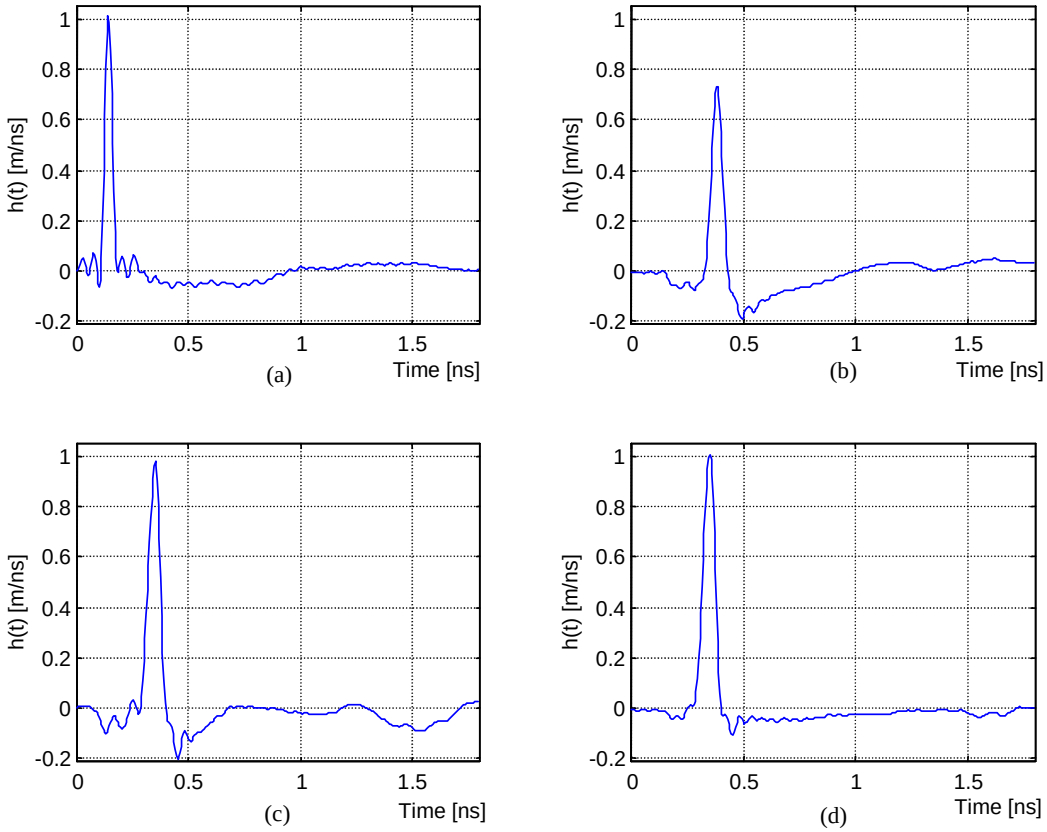

Figure 5: (a) $h_N(t)$ of antenna 1 (b) $h_N(t)$ of antenna 2 (c) $h_N(t)$ of antenna 3 (d) $h_N(t)$ of antenna 4

For a detailed comparison of the antennas, we summarise some important characteristics of the normalised IR in Table 4.2, i.e. the maximum value of the normalised IR, the full width at half

maximum value (FWHM) of the impulse, the area under the impulse, and the tail fluctuation as a portion of the maximum value.

	Max of $h_N(t)$ [m/ns]	FWHM [ps]	Area under impulse [m]	tail fluctuation [% of max]
Antenna 1	1.01	38	0.038	13%
Antenna 2	0.73	56	0.041	33%
Antenna 3	0.98	60	0.059	22%
Antenna 4	1.01	60	0.062	11%

Table 4.2: Important characteristics of the normalised IR

The FWHM value of the normalised IR is related to the bandwidth of the antenna. The area under the impulse is related to the effective antenna height [9]. It can be seen that filling the antenna with the dielectric reduces the bandwidth, but increases the area under the impulse. The presence of the absorber material at the end of the antenna plates of antenna 4 has a positive influence on the antenna performance. The comparison with antenna 3 shows that the absorber material does not affect the bandwidth nor the area under the impulse, but it considerably decreases the fluctuations in the tail of the response. Thus antenna 4 will be capable of radiating transient pulses with less ringing. It would be difficult to demonstrate this antenna property with the classical frequency domain characterisation of an antenna.

5. TIME DOMAIN SIMULATIONS USING THE NORMALISED IR

The normalised impulse response is a powerful tool that can be used for simulation and system design purposes. Some examples are presented in this section. For each example the simulated data are compared with measured data. The antenna used in the simulations is antenna 4 described in the previous section.

A. Two antennas on boresight

The first simulation is straightforward. Two antennas are put on boresight at a distance of R = 90 cm. A very short transient impulse with a maximum amplitude of 2.5 V in a 50 Ω load and a FWHM of 90 ps is used as a driving voltage V_s (Fig. 6a).

The transient voltage signal V_{rec} at the output of the receiving antenna is calculated using (2.7) and measured using a digitising oscilloscope. Figure 6b shows the calculated waveform and the measured waveform. Both time and voltage data of the two waveforms correspond well.

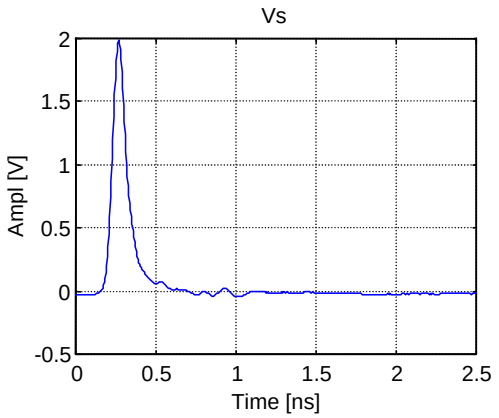

Figure 6a: Driving signal V_s

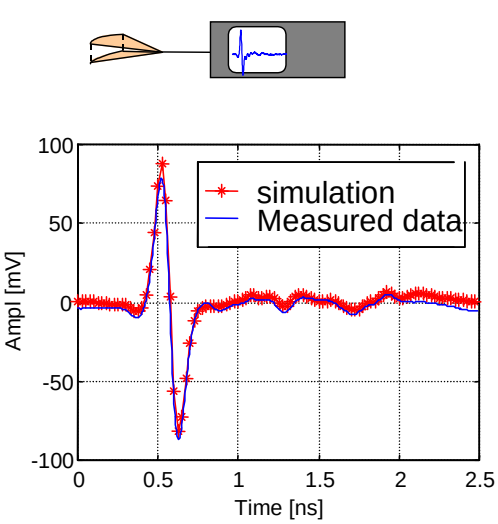

Figure 6b: Two antennas on boresight, simulated and measured data

B. Reflection on a planar air-ground interface

In a second example the reflection on a planar dry sand interface is simulated. The bistatic configuration, typical for ground penetrating radar, is represented in Figure 7. The two antennas are focused at a point on the interface. The distance between the virtual sources of the TEM horns is 22.8

cm. The H-field polarisation of the antennas are in the same plane, the E-field polarisation of both the antennas is parallel to the interface. The driving voltage V_s is the same as in the previous simulation.

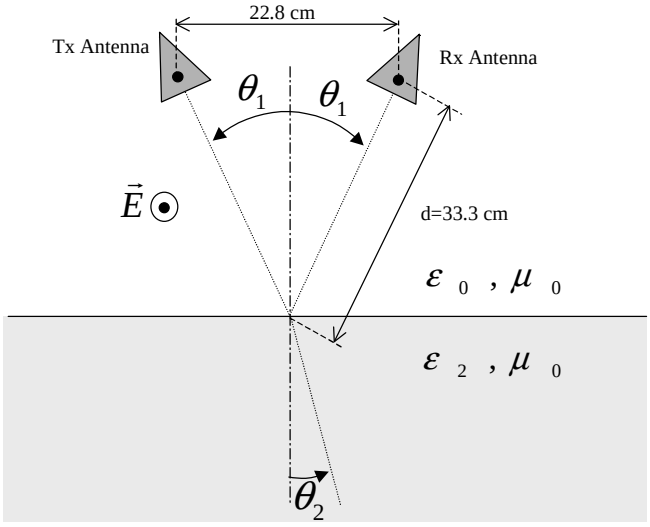

Figure 7: Bistatic configuration

The dry sand is characterised by an ε_r of 2.55 and an μ_r of 1 in the frequency band of interest, and is assumed to be homogeneous and lossless. The reflection coefficient for parallel polarisation is given by $\Gamma_A = \frac{\sqrt{\varepsilon_0}\cos\theta_1 - \sqrt{\varepsilon_2}\cos\theta_2}{\sqrt{\varepsilon_0}\cos\theta_1 + \sqrt{\varepsilon_2}\cos\theta_2}$, which is - 0.248 in this case. The total path loss in the simulation is due to the free-space loss over a distance 2d and to the reflection loss from the air-sand interface. The simulated data is obtained by multiplying the result of (2.7) by Γ_A. Despite the fact that the air-sand interface is near the antennas, the result of the simulation is very similar to the measured data (Fig. 8). Note that the direct coupling between transmitting and receiving antennas, which is not taken into account in the simulation, will also introduce errors.

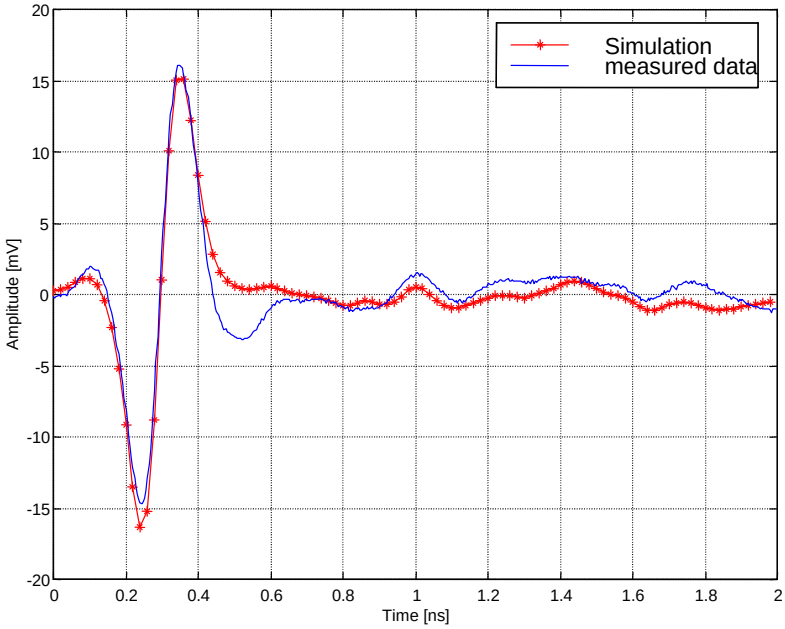

Figure 8: Reflection on a planar dry sand interface, simulated and measured data

C. The echo of a metallic disc

In the last simulation, the normalised antenna equations are used in combination with commercial FDTD software. The bistatic antenna configuration, almost the same as in the previous example, is represented in Figure 9. An aluminium disc with a radius of 3.2 cm and 1cm thick is placed at the focus point of the two antennas.

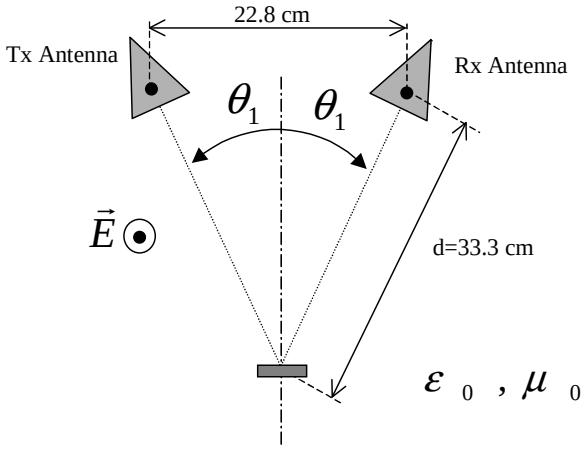

Figure 9: Bistatic configuration for metallic disc

Expression (2.5) is used to calculate the radiated E-field at the metallic disc. This wave, assumed to be planar, is introduced in a FDTD programme, which calculates the backscattered field at a point

corresponding to the virtual source of the receiving antenna. Using this backscattered field as an incoming field for expression (2.6), we calculate the received voltage at the output of the receiving antenna. The simulated data and the measured data are given in Figure 10. Again, the correspondence is good. An advantage of this simulation scheme is that we do not need to model the antennas in the FDTD programme.

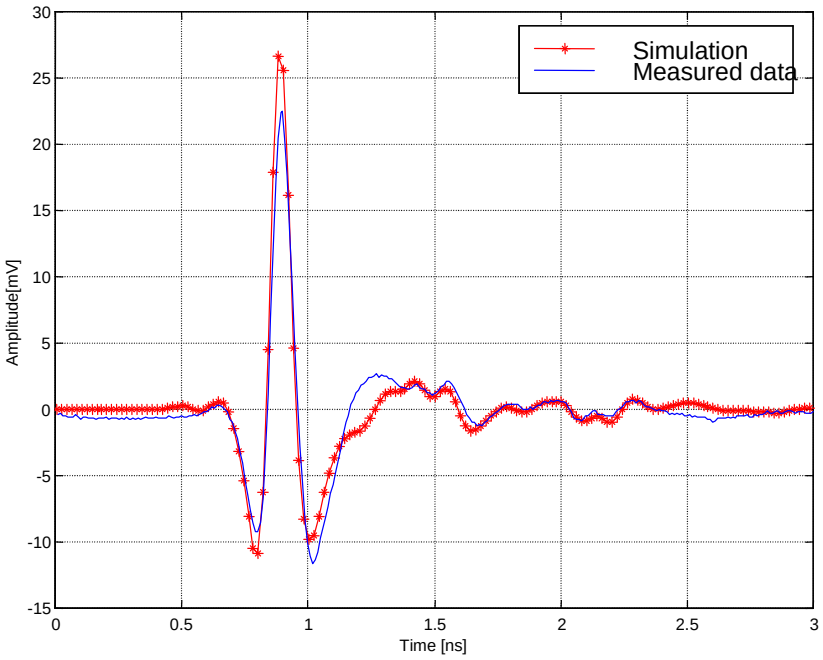

Figure 10: Echo of a metallic disc, simulated and measured data

6. CONCLUSIONS

The normalised IR describes time domain antenna performances, which are sometimes difficult to see in classical antenna parameters, in a compact way. The advantage of using the normalised IR over any other impulse response is that all frequency dependent characteristics are included in the normalised IR. This has two important consequences. First, the time-domain antenna equations become very simple and accurate to use, without any assumptions about antenna impedance. Second, the normalised IR permits a comparison between different variants of time domain antennas, taking into account all these frequency dependent terms.

It has been shown that the normalised IR is easy to measure, using two identical antennas and a vector network analyser. Due to the finite but non-zero size of the antenna, the distance from an observation point to the antenna becomes ambiguous for points close to the antenna. The introduction of an apparent point in the antenna, called the virtual source - which can be seen as the origin of the radiated impulse TEM wave - resolves this shortcoming. The position of the virtual source in the antenna can easily be located.

Thanks to the introduction of the virtual source the antenna equations can now be used near the antenna. This is clearly shown in the examples of the time domain simulations. The examples also demonstrate the simplicity and accuracy of the time domain simulations, using the normalised IR. Such simulations can also be applied for simulating system performance with e.g. different transient impulse generators or for radar range estimation.

Although the antenna equations and the normalised IR are limited in this paper to antennas on boresight and to dominant linear polarisation of the E-field, the extension to the more general case is possible and will be considered in the future.

7. REFERENCES

[1] M. Kanda: *Time-Domain Measurements in Electromagnetics*, Edited by E. K. Miller, Van Nostrand Reinhold Company Inc, New York, 1986, chap 5, p 122-174.

[2] R.L. Carrel: 'The Characteristic Impedance of Two Infinite Cones Of Arbitrary Cross Section', *IRE Trans. on Antennas and Propagat*.,1958, AP-6, pp. 197-201.

[3] M. Kanda: 'Transients in a Resistively Loaded Linear Antenna Compared with those in a Conical Antenna and a TEM Horn', *IEEE Trans. Antenna Propagat.*, Jan. 1980, vol. AP-28, no. 1, pp. 132-136.

[4] M. Kanda: 'The Effects of Resistive Loading of TEM Horns', *IEEE Trans. Electromagnetic Compatibility*, May 1982, vol. EMC-24, no. 2, pp. 245-255.

[5] A.P. Lambert, S.M. Booker and P.D. Smith: 'Transient Antenna Design parameters for optimising Radiated Pulse', AGARD, Electromagnetic Wave Propagation Panel, Proc. 54th Specialists' Meeting on High Power Microwaves, Ottawa, Canada, May 1994, Chapter 8.

[6] J.F. Aurand: 'A TEM-Horn Antenna with Dielectric Lens for Fast Impulse Response', *Ultra-Wideband, Short-Pulse Electromagnetics3*, Edited by Baum et al., Plenum Press, New York, 1997, pp.113-120.

[7] B. Scheers, M. Piette, A. Vander Vorst: ' Development of Dielectric-Filled TEM Horn Antennas for UWB GPR', submitted to IEEE AP-2000 conference, Davos, Switzerland, April 2000.

[8] E.G. Farr and C.E.Baum: 'Extending the Definitions of antenna gain and Radiation Pattern Into the Time Domain', Sensor and Simulation Notes, note 350, 1992.

[9] E.G. Farr and C.E.Baum: 'Time Domain Characterization of Antennas with TEM Feeds', Sensor and Simulation Notes , note 426, 1998.

[10] C.E.Baum: 'General Properties of antennas', Sensor and Simulation Notes, note 330, 1991.

[11] A.V. Oppenheim, R. W. Schafer: *Digital Signal Processing*, Prentice-Hall, New Jersey, 1975